13 The basic design of the dual thin film probe for total temperature measurements applied in low frequency periodic flow at ambient static conditions

13.1 Introduction

The operating principle of the dual thin film probe as well as several applications of the probe in high speed flow are widely discussed in chapters 11, 12 and will be discussed in chapters 14, 15. In this chapter, the probe is also tested at quite different flow conditions such as low Mach number and ambient temperature. It is placed behind a nozzle designed for uniform flow conditions and the time-averaged total temperature calculation results are compared with thermocouple measurements. At the same time, a disc with three 'openings' that turns at low RPM is located between the nozzle and the probe. The probe feels periodically the flow, each time it is behind an opening. The phase locked average on the wall temperature signals is examined for a very low number of periods.

13.2 Description of the set up generating the low frequency periodic flow

The dual thin film probe is placed in a fixed position behind a nozzle with uniform exit conditions not further than one diameter from the nozzle exit (*32mm*) (Figure 13-1). A fast response thermocouple is placed just under the probe. A disc with three 'openings' is placed between the nozzle exit and the probe. It is connected to an electrical motor and can turn at constant speed. The flow from the nozzle is applied on the probe and the thermocouple only when it passes through one of the three openings. A shutter is also placed just in between the nozzle and the disc. Once the set up is mounted, the closed shutter deflects the flow at the exit of the nozzle, the probe is heated and the disc starts turning. When the disc reaches the required rotational speed, the shutter opens and the probe feels periodic steps in gas temperature, every time it is behind an opening. The exit Mach number is between *0.038* and *0.075* and the gas temperature is equal to the ambient temperature.

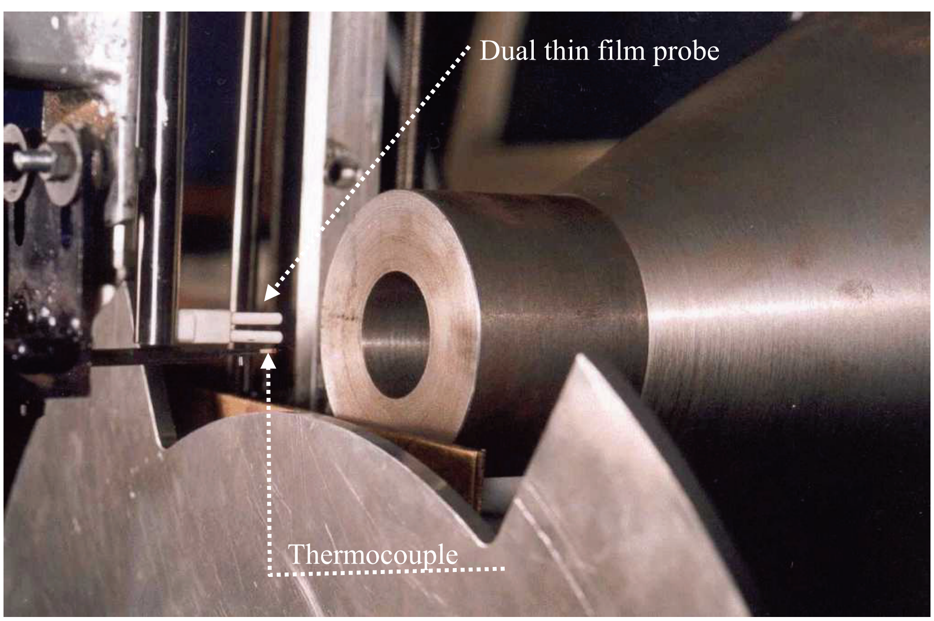

Figure 13-1: Set up of the periodic flow: the D.T.F.P. behind one of the three 'openings' of the disk and the nozzle with the uniform exit flow

As the measured total temperature is the ambient one, there is no need for high heating of the probe ceramic heads, because in low heating cases, the wall temperature of the cold head is not far from ambient temperature. Thus, the basic design of the probe using a Plexiglas or Ertalon support can be successfully used for the next series of measurements.

13.3 Measurements behind a nozzle

13.3.1 Measurement chain

The sensitivities of the two gauges (of the Plexiglas support probe used for the next measurements) and of the Wheatstone bridges are given in Table 13-1. The sampling frequency is *5kHz*. The periodicity of the signals is around *33Hz* and thus, the time-averaged component is numerically generated by low pass filtering the voltage signals at *10Hz*. The time-resolved component is also numerically generated by high pass filtering the same voltage signals at *10Hz*. Then both components are transformed to wall temperatures and a PLA of *20* periods is performed on the time-resolved component based on the disc openings passing frequency. The equivalent wall heat fluxes are then calculated. Finally, time-averaged and time-resolved wall temperatures and heat fluxes are added in the time domain for the gas temperature calculation. (More detailed description in Figure 14-8 of paragraph 14.3.2.1).

Gauge	Resistance Thermometer	Wheatstone bridge
Hot	$T_{W1} = 13.149\ R_1 - 430.91$	$d_R/d_V = 1.6466$
Cold	$T_{W2} = 13.288\ R_2 - 426.53$	$d_R/d_V = 1.4622$

Table 13-1: Measurement chain: sensitivity of the gauges and the Wheatstone bridges for each gauge of the Plexiglas support D.T.F.P. in the low frequency periodic flow

13.3.2 Periodicity and PLA on the wall temperature signals

The Fast Fourier Transform (FFT) of the time-resolved wall temperature of the hot head is shown on the top graph of Figure 13-2. The resolution in frequency is *1.2Hz* and the signal is high pass filtered at *10Hz*. The harmonic of the disk opening passing frequency (at *33Hz*) is clearly visible. However, the second highest peak in magnitude (which is also of the same order of the highest peak) is at *100Hz* and not at *66Hz* (that corresponds to the second harmonic). A closer look to the frequency axis more peaks are visible. Apparently, there are two main frequencies that described the wall temperature signal: one at *33Hz* and one at *100Hz*, three times higher. The rest of the peaks are combinations of the harmonics of the two main frequencies. Note that although the *100Hz* peak could also contain frequencies coming from the electrical network noise (*99-100 Hz*), because there is not a high peak at *50Hz*, this noise contribution on the *100Hz* peak seems negligible. Moreover, the probe was well attached to the support that did not move and thus, no mechanical frequencies are expected on the wall temperature signals. To conclude the second highest peak in magnitude at 100 Hz is part of the signal and is not generated by the electrical noise.

The phase locked average (PLA) is performed on the wall temperature fluctuations generated by high pass filtering the signals at *10Hz*. It is shown as a function of the openings passing phase $\Phi_{disk/3}$ on the bottom graph of Figure 13-2. For the time period $\Phi_{disk/3} = 0$ till $\Phi_{disk/3} = 1$, the disk performs an angular displacement equal to the pitch of one opening and one closed part of the disk, which corresponds to $(360/3)° = 120°$. The number of periods is *20*. The hot head fluctuation range reaches $\pm$ *0.6K* (ΔT_{W1}) whereas the cold head fluctuation range is only *0.15K* (ΔT_{W2}). [These fluctuations are one order of magnitude higher compared to the PLA fluctuations from the experiments of the probe behind the rotor of the one and a half stage turbine (Figure 14-11). Thus, the low frequency of the periodic fluctuations requires no special amplification of the acquired temperature signals as a function of $\sqrt{j\omega}$ (see also paragraph 4.3.4)].

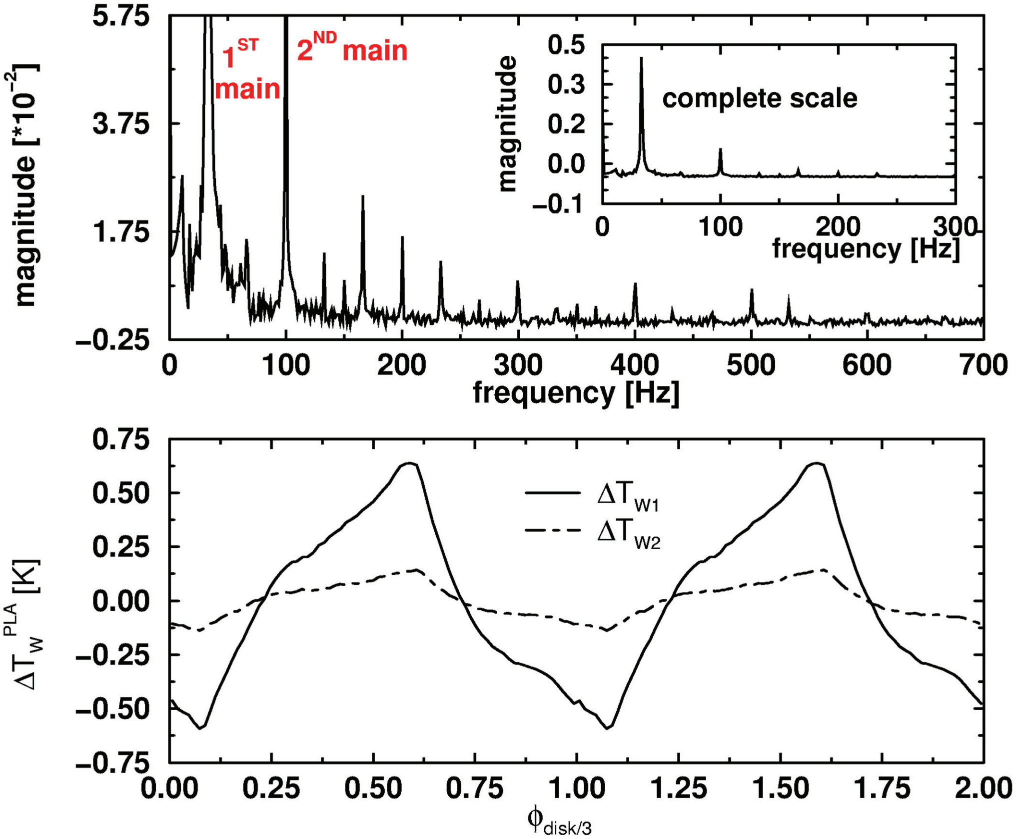

Figure 13-2: FFT on the wall temperature fluctuations of the hot head (ΔT_{W1}) at the top and PLA on both heads fluctuations at the bottom for test 1 (Plexiglas support D.T.F.P. in the low frequency periodic flow)

A better look on the PLA wall temperature fluctuations also illustrates that the *100Hz* frequency appearing on the FFT of the above signal is a main frequency and not a harmonic. At openings passing phase $\Phi_{disk/3}$ between *0.30* and *0.55*, although the wall temperature still decreases, this fall is less strong than just before, while at $\Phi_{disk/3}$ between *0.75* and *1.0*, the increase is less strong than just before.

The above argument would have been reinforced, if the pressure had also been recorded at the position of the probe behind the disk. The only additional information is that the opening width is three times larger than the jet diameter. (Also note that the *100Hz* frequency is three times higher than the one of *33Hz* that corresponds to the disk opening passing frequency.)

It could be assumed that when the opening starts to uncover or to cover the nozzle diameter, the air pressure at the stagnation point of the heads could be different than the pressure when the opening lets the jet air to freely pass through. These possible pressure changes on the heads probably generate the 100Hz frequency on the temperature signals.

The repeatability of the PLA is shown for four different tests in Figure 13-3. The nozzle exit Mach number for the test 1 described in Figure 13-2 is *0.038*, the same as the test 3. The

Mach number for tests 2 and 4 is *0.075*. The average disk opening passing frequency is *32.5 ± 0.7Hz*.

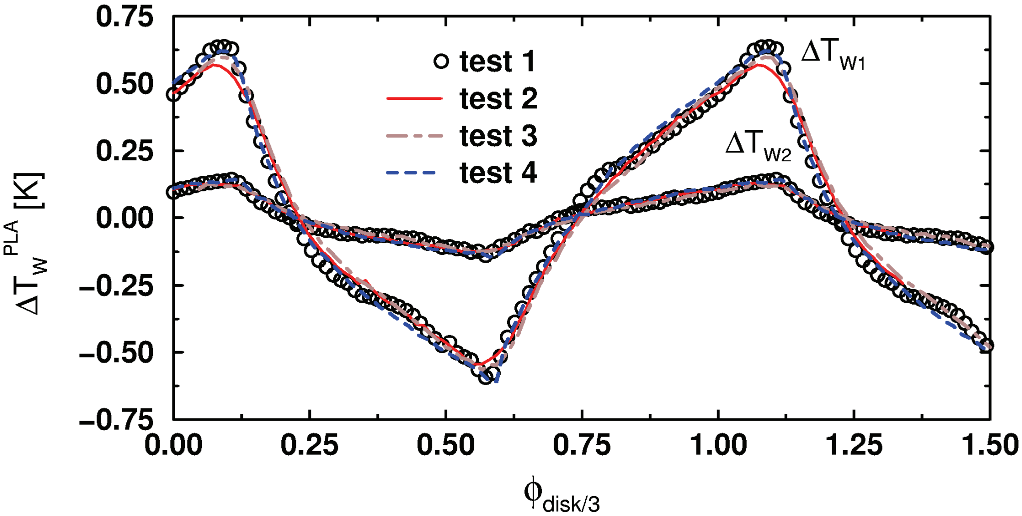

Figure 13-3: Repeatability of the PLA on the wall temperature fluctuations for both heads (Plexiglas support D.T.F.P. in the low frequency periodic flow)

Test 1 is described, in Figure 13-4: on the three left graphs, the fluctuations are added to their corresponding time-averaged component in the time domain, while on the three right graphs, only the time-averaged components are presented. The wall temperatures are illustrated on the top graphs and their corresponding heat fluxes on the bottom graphs. The two middle graphs compare the gas temperature calculations with a fast response thermocouple.

More into detail, the initial wall temperatures are very low (top-right), because the heating was also very low. However, this temperature difference of *32.7 K* is high enough to calculate the average gas temperature (middle-right), as the cold head wall temperature is close to the one of the flow and the velocity not high enough to quickly cool down the hot head. The difference with the thermocouple was *2* to *3 K*, something that was observed for all the tests. Thus, the accuracy of the probe compared to the thermocouple seems to be better than *3 K*. On the other hand, it is possible that a more careful determination of the initial wall temperatures just before the shutter opens can eventually improve the accuracy of the probe. For these cases, the resistances of the thin films were manually measured to determine the initial wall temperatures, a bit before the shutter opens. However, it would be better that the Wheatstone bridges that can operate into two modes should have been used (chapter 14.2), because the head temperatures were strongly influenced by the rotation of the disk just prior to the test. Note that the main functions of the two modes are:

(i) the determination of the overall initial resistance just prior to the test,

(ii) the acquisition of the resistance variations with time,

The two modes Wheatstone bridges were used for the tests performed behind the rotor and the second stator in the one and a half stage turbine CT3 facility; while the thin film resistances were measured just prior to the tests behind the high speed cascade in CT2 facility (chapters 11, 12).

It should be also pointed out that when one of the two wall initial temperatures is brought close to the expected gas temperature, a *30 K* difference between the two heads is sufficient for the gas temperature calculations. The same conclusion can be drawn from the tests behind the cascade in CT2 facility (see Figure 12-7). Lower initial temperature differences between the two heads introduce high noise and thus high uncertainty on the gas temperature calculations.

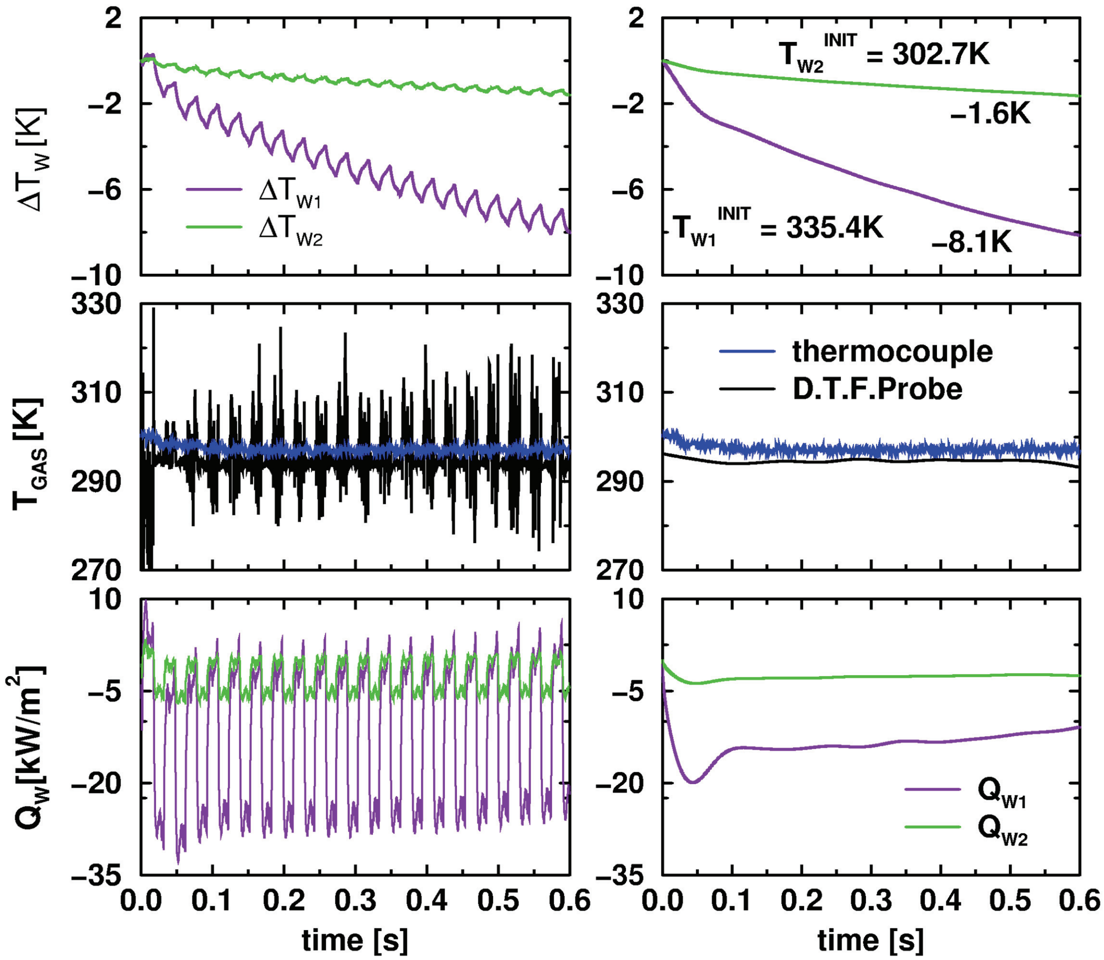

Figure 13-4: On the left the total and on the right the time-averaged wall temperatures (top), gas temperature (middle) and wall heat fluxes (bottom) for PLA on 20 periods (test 1) (Plexiglas support D.T.F.P. in the low frequency periodic flow)

Moreover, each time that the probe is hidden by the disk, both wall heat fluxes (bottom-left) reach values close to zero. (Theoretically, on one hand, there is natural convection that continuously cools down the two heads, on the other hand the heating in the probe remained on during the test and heats up the heads. These two phenomena generate wall heat fluxes of one order of magnitude smaller than the ones measured when the probe feels the jet air. This is the reason that the measured wall heat flux for each head is almost zero.) Thus, no gas temperature calculations are possible during this time (middle-left). Only high noise is generated that has no physical significance.

Figure 13-5 is similar to Figure 13-4 and describes the test 2. The PLA is performed on *40* periods (till *1.2s*). (The change in the number of periods compared to the test 1 enforces the reliability of the results shown for *20* periods.) The noise on the wall heat flux for the results of 40 periods is smaller mainly for the hot head (bottom-left).

It is important to be mentioned that even if the heating was higher (thus higher initial wall temperature differences), when the probe is out of the flow, both heat fluxes still reach almost zero values and the gas temperature calculation is still not possible.

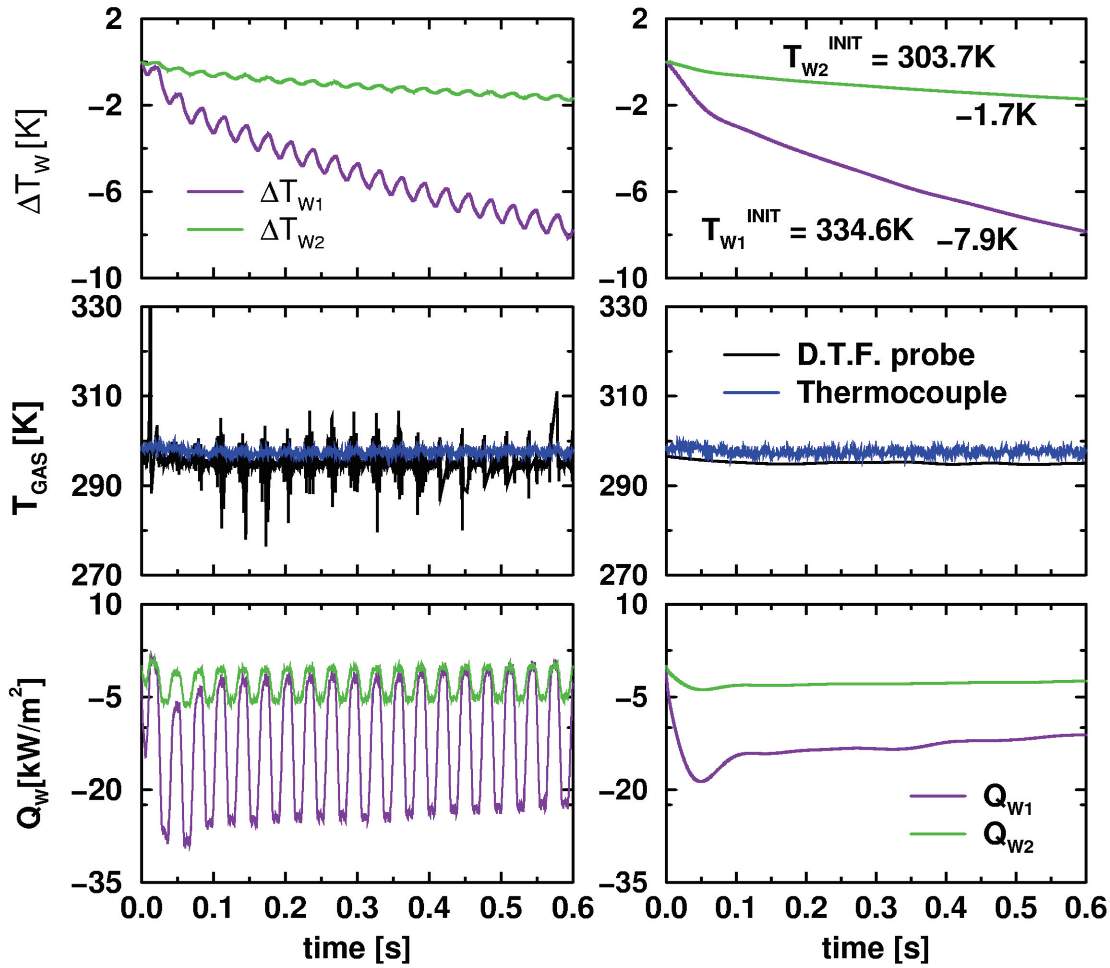

Figure 13-5: On the left the total and on the right the time-averaged wall temperatures (top), gas temperature (middle) and wall heat fluxes (bottom) for PLA on 40 periods (test 2) (Plexiglas support D.T.F.P. in the low frequency periodic flow)

13.3.3 Uncertainty analysis

An error analysis on the gas temperature results of the dual thin film probe requests an error analysis on the wall temperatures as well as on the wall heat fluxes. The uncertainty on the wall temperature is calculated equal to *0.05K*. However, an error analysis on the wall heat flux is not applicable: after the conduction equation is numerically solved inside the gauge substrate, the wall heat flux is calculated through the Fourier law. Thus, the necessity of comparing the results of the dual thin film probe with the results of other well validated instruments is of great importance for an estimation of the probe uncertainty.

The uniform air jet flow is characterized by the least flow perturbations compared to the flows in the isentropic light piston tunnels. Thus, the comparison of the probe results with the thermocouple or cold wire results under the air jet flow can give a good estimation of the uncertainty of the probe results. The previous measurements showed a difference with the thermocouple results of *2* to *3 K*.